Cell Responses on micro-patterned substrate

Introduction

Tissue engineering, often used synonymously with the term regenerative medicine, applies in the repair of replacement of whole tissues. This is a significant research aspect in medicine, for it has the potential to develop biological substitutes that restore, maintain, or improve tissues or even a whole organ. These applications usually require cells to be specifically placed to generate organized structures such as a neural network and liver system. When studying these cells *in vitro* however, it is difficult to completely mimic an *in situ* environment. When extracellular matrix play an essential role for many cell processes such as proliferation and differentiation, studying cells under *in vitro* environments would yield erroneous results when applied to situation with human subjects. One way to overcome this is to grow a monolayer of cells to coat the scaffold surface. However, endothelial cell adhesion is usually poor when the cells are pre-seeded onto artificial biomaterials under static conditions as the standard cell culture protocol. In response to this, creating a new type of microfluidic device to study the functions of the individual cells and cell-cell interaction, and how cells could be controlled to proliferate is essential.

In previous studies, it has been reported that cells align themselves along the shear flow direction. The interaction of endothelial cells with fluid flow was studied in hopes to develop conditions where a stable endothelial monolayer could grow. In addition to this study, another study had the same intentions and studied the spread and alignment of cells cultured *in vitro* on a grooved polymer surface. It was reported that the cells aligned themselves along the grooved, wavy surface. By Combining the two results and creating a microfluidic device with a wavy surface where the cells are exposed to shear flow, a new perspective on how cells respond to *in vitro* environments can be recognized. This experiment assesses the preliminary steps in creating such a device. Human Lung Endothelial cells are exposed to substrate with two patterns: micro-wave and micro-groove. The cell proliferation, spread, and alignment angle is quantified using images captured by a phase-contrast microscope and analyzed with imaging software, ImageJ. From these results, the type of surface utilized for a microfluidic device may be determined. It is hypothesized that the micro-wave pattern would have better control of the cell's positions due to the gradual change in topography and the greater exposure to cell medium.

Materials and Methods

In hopes to successfully characterize cell growth and responses on micro-patterned PDMS substrate, Human Lung Endothelial (HLE) cells were seeded onto a micro-wave and micro-groove PDMS substrate. The cells were then observed under a phase-contrast microscope, permeabilized and applied with primary antibody for actin-stained image recording by a confocal laser scanning microscope.

Micro-patterned PDMS Substrates

PDMS was chosen for the substrate material due to its ease in micro-pattern fabrication at low cost and excellent biocompatibility and mechanical properties [42]. The micro-wave pattern was created with a wavelength of 20μm and a height of 6.6μm. Two micro-groove patterns were created with 10μm

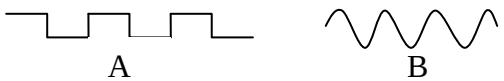

Fig..
Cross sections of the micro-patterned PDMS substrate A) micro-groove B) micro-wave

spacing and 5μm height, and 20μm spacing and 6.6μm height.

Cell Culture

HLE cells were maintained in cell culture flasks that were kept at 37°C in Dulbecco's Modified Eagle's medium (DMEM) containing heat inactivated Fetal Bovine Serum (FBS) and 1% Penicillin/Streptomycin that was retained at 100% humidity. Determined by a hemocytometer count, approximately 2-6 x 10^5 cells/mL concentrated cells were seeded by standard cell culture protocol onto the micro-patterned PDMS substrate. After 24 hours and 48 hours of incubation, cell spreading and orientation was then imaged with a Nikon phase-contrast microscope 20x.

Actin Filament Immuno-fluorescence Staining

The distribution of actin filament plays a significant role in the shape, alignment, and spread of the cells. After 24 and 48 hours of cell incubation on the micro-patterned PDMS substrates, the cells were fixed with 3-4% paraformaldehyde for 10-20 minutes, rinsed with Phosphate Buffer Solution (PBS), and permeabilized with 0.5% Triton X-100 for 2-10 minutes [43-44]. Primary antibody was then applied to the micro-patterned PDMS substrate with the cells, and incubated for 60 minutes at 25°C room temperature. After three thorough rinsing with PBS, the stained cells on the micro-patterned PDMS substrate were imaged under a confocal laser scanning microscope.

Modeling Cell Adhesion

Using a 18μm diameter model sphere, a single suspended cell is modeled by Link180 3-dimensional element. Based on a previous study by McGarry et. al (2004), a tensegrity structure with a height of 14μm attached to the sphere then represents the cytoskeleton indicated by the six struts and twenty cables employed as the microtubules and microfilaments respectively. The material properties were obtained by the previous study by McGarry et. al.: linear elastic modulus was $1.2x10^9$ and $2.6x10^9$ Pa for microtubules and micro filaments respectively, and Poisson's ratio was 0.3 for both components. The six struts were assumed to be rigid without possibility to buckle. Three bottom nodes were constrained: node 1 was constrained in x, y and z direction, node 2 was constrained in y and z direction, and node 3 was constrained in y direction. In the model, a cross section and length of $1x10^{-12}m^2$ and 15.48μm, respectively, were used for the strut; a cross section and length of $1x10^{-14}m^2$ and 9.8μm were used for the tension cables. After applying a tensilfe force of 1nN, the strain energy and stiffness of the cell among the three surface geometries (flat, concave, convex) is compared to observe the effect of surface geometry on cell adhesion.

Preliminary Results

Micro-wave Pattern

Cell Distribution

To quantify the cell distribution, the 20μ wavelength was divided into 1μm segment locations and a histogram of the number of cells in each segment was created (Fig. 1). After initial seeding, the HLE cells were almost uniformly distributed on the wavy surface, favoring the troughs of the waves over the crests. In the phase-contrast microscope image, the white lines represent the crest of the micro-wave surface. Comparing the images captured after 24 hours and 48 hours, no significant differences were observed on the distribution or spread of the cells as seen in figures 1-3; thus, the incubation time of 24 hours was utilized for further analysis. After

incubation on the micro-wave PDMS substrate, the majority of the cells were still located at the troughs of the waves.

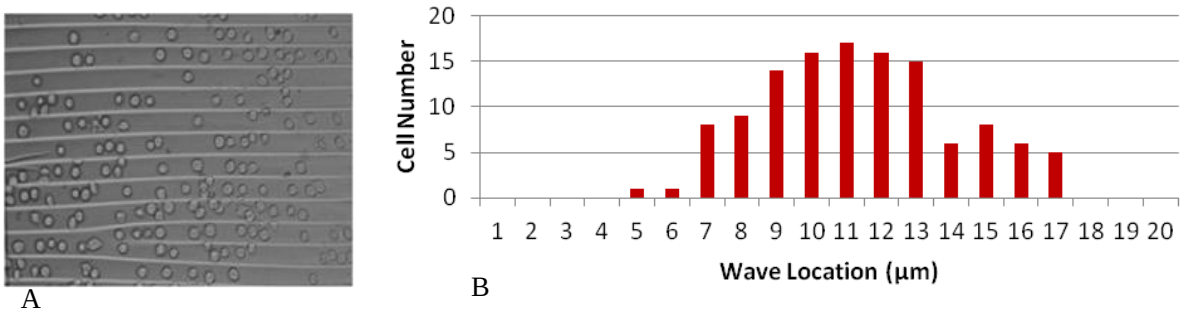

Fig. 1.. A) Phase-contrast image after initial seeding of HLE cells; B) Histogram of HLE cell number at different wave locations

Cell Spread and Alignment Angle

The alignment angle is defined as the angle between the long axis of the cell, and the wave direction. extent of the cell alignment was quantified using imaging software Image J. About 60% of the cells had a <10° alignment angle, with a significant fraction of them very close to 0°. A wider angle distribution of cells is observed at the troughs while a narrower angle distribution is observed at the crests. The HLE cells spread along the troughs or crests, or the wave direction, of the micro-wave surface; whereas the in the control, where cells were seeded on a flat PDMS substrate surface, the cells appeared to be rounder and more randomly oriented. About 50 cells were measured and a statistical analysis was performed using excel.

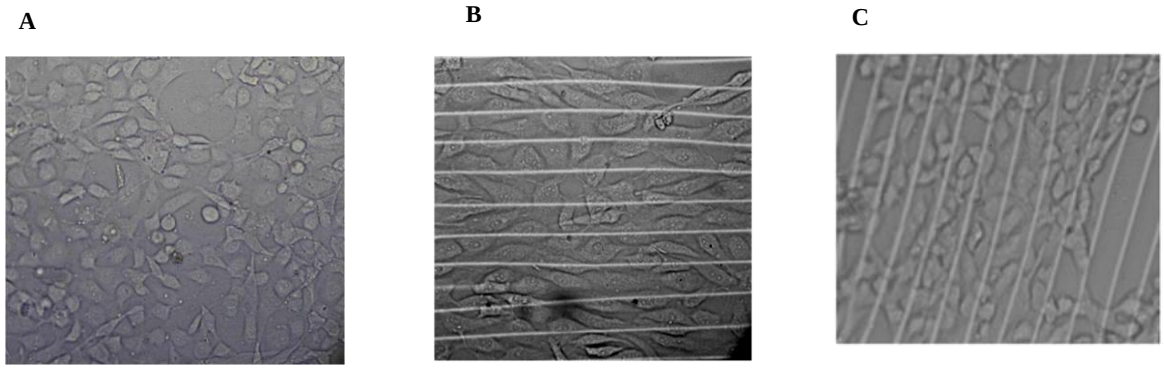

Fig. 2 . Phase-contrast images of HLE cells at[magnification here] after incubation (A) Control 24h; (B) Micro-wave after 24h; (C) Micro-wave after 48h

Cell Death

Determined by a live/dead stain, the cells at a death rate of 25% after 24 hours.

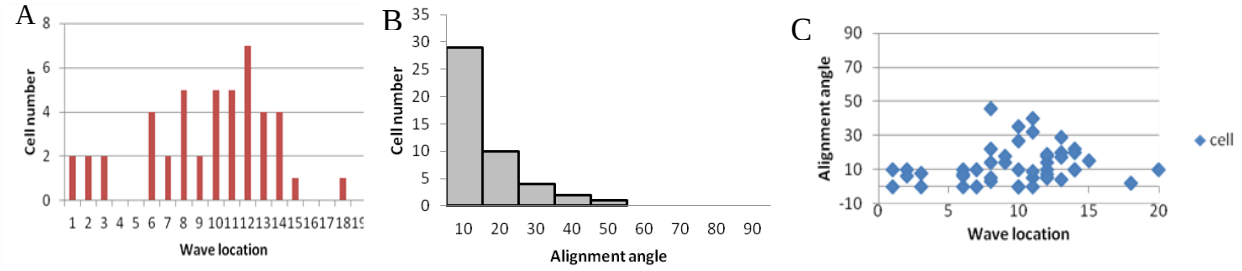

Fig. 3. HLE cell A) wave location; B) histograms of alignment angle; C) Alignment angle in terms of wave locations

Micro-grooved Pattern

Physical Attributes of the Cells

Similarly to the micro-wave pattern, most of the HLE cells were located at the troughs of the grooves both at the initial seeding and after 24 hours of incubation. The 20m spacing micro-groove pattern, there was at 35% death rate after 24 hours. Cells on the 10m spacing micro-groove pattern had a 55% death rate.

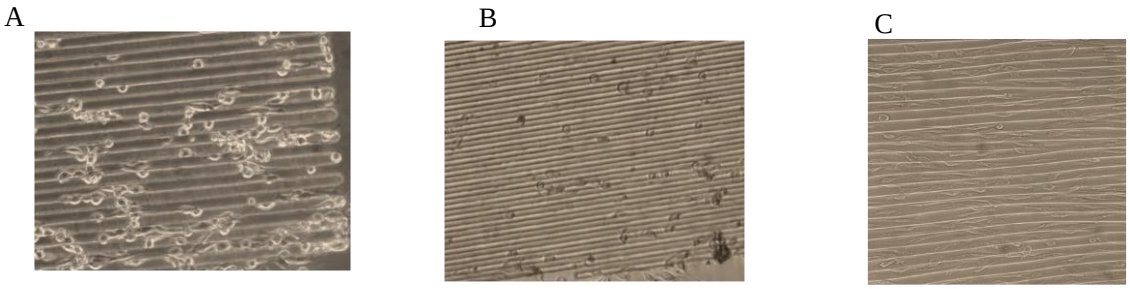

Fig. 4. Phase-contrast images of HLE cells after 24h incubation: A) 20µm spacing, 5µm height micro-groove; B) 10µm spacing, 5µm height micro-groove; C) 20 m wavelength micro-wave

Finite Element Analysis(FEM)

Using a 18µm diameter model sphere, a single suspended cell is modeled by Link180 3-dimensional element. Based on a previous study by McGarry et. al (2004), a tensegrity structure with a height of 14µm attached to the sphere then represents the cytoskeleton indicated by the six struts and twenty cables employed as the microtubules and microfilaments respectively.

By modeling nodes 1-3 anchored to the substrate surface and moving the nodes 7-9 vertically, the cell spread shape may be mimicked, dependent on the surface geometry rather

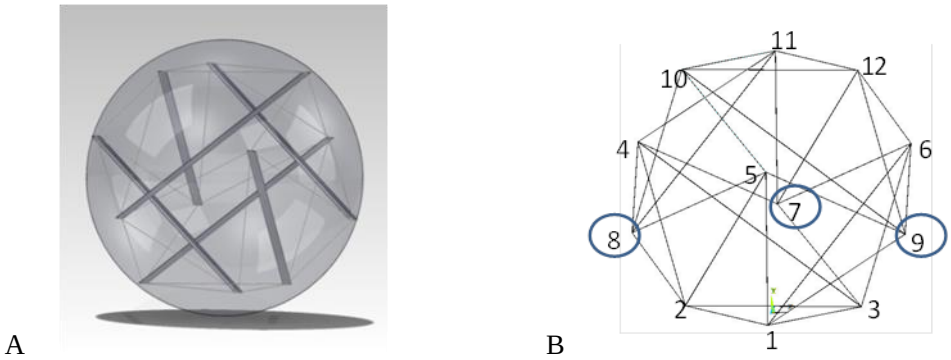

Fig. 5. Cell model (A) sphere including a tensegrity structure; (B) tensegrity structure

than the micro-pattern. On the control, a 5µm displacement was utilized. The concave displacement was 3µm while the convex displacement was 7µm.

After an application of 1nN tensile force, the stiffness and strain energy was calculated using the obtained displacements.

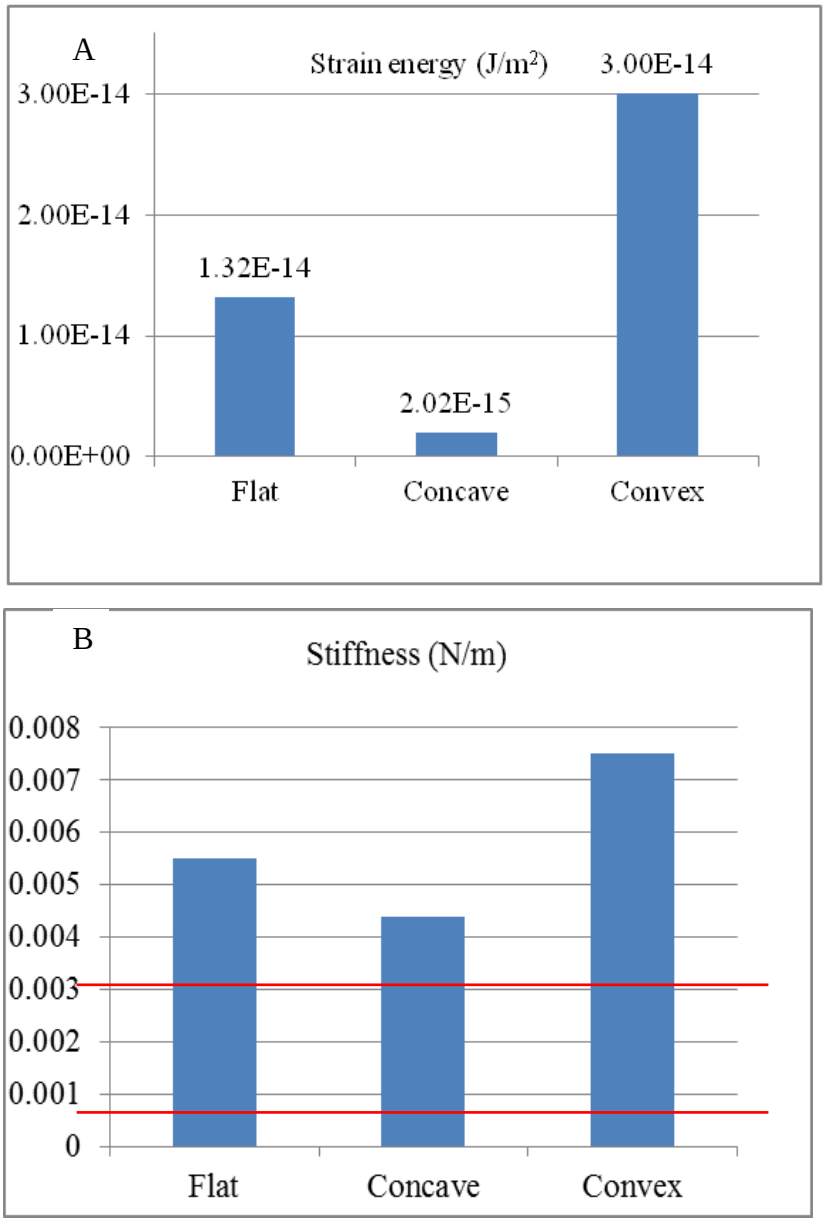

Fig. 6. Calculation for the three geometries (flat, concave, convex) based on the displacement obtained through finite element analysis via Link180 3-D elemtn, the calculation of A)Total strain energy; B) Stiffnesss

Brief Discussion/Future Work

By seeding HLE cells on micro-wave and micro-groove patterned PDMS substrate, the influence of micro-patterns on the physical attributes of the cells and cell functions are observed. The cell distribution after 24 hours was visualized by a phase-contrast microscope in addition to cell alignment angle calculations done by an imaging software. The cell death rate was also calculated in hopes to understand the effect of the substrate pattern on biosafety. Overall, it was determined that the micro-wave pattern better control the proliferation, spread and alignment of

the cells; therefore, the micro-wave pattern will be utilized to proceed to further testing in flow and modeling.

Flow testing

In our research, we apply endothelial cells on to the PDMS micro-wave surface. Culture of endothelial cells in vitro is usually performed under static conditions such as in a culture dish or flask with stationary medium; however, endothelial cell adhesion is usually poor when the cells are pre-seeded onto artificial biomaterial under static condition. Since endothelial cells form the inner lining of blood vessels, they are normally exposed to continuously flowing blood, even during blood vessel development (angiogenesis). It is therefore desirable to study the cell/biomaterial interactions in vitro under conditions closely resembling those in vivo, specifically under shear stress.To further improve the patterns of cell distribution and orientation, external stimuli such as shear flow and cyclic strength could be applied through a syringe pump. To investigate adhesion strength, attached cells are subjected to increasing levels of flow-induced shear stress over a 12 min period. Culture medium is dispensed using a syringe pump (Harvard Apparatus series 11, Harvard, Holliston, MA, USA) at 12 mL h^{-1} for the first 4 min, 120 mL h^{-1} for the next 4 min, and 240 mL h^{-1} for the final 4 min. These flow rates translate to shear stresses of 11, 110, and 220 dyn cm^{-2}, respectively.

Two control experiments will also be performed to examine how quickly cells detached over time, and to evaluate whether initial low shear stress levels preconditioned cells for detachment at higher shear stresses in the approach outlined above. The first experiment comprised repeating the standard shear assay of 11, 110, and 220 dyn cm^{-2} at 4 min intervals and capturing images every 30 s over the 12 min period to obtain intermediate time points. The second experiment comprised applying 220 dyn cm^{-2} for 12 min, also with images captured every 30 s. Results are presented for experiments performed with PAVECs on 50 mg mL^{-1} FN. Similar results are observed with other combinations of cell type and coating concentration.

Uniaxial Cyclic Stretch

A uniaxial sinusoidal stretch of 20% in strain at 30 cycle/min was applied using stretching apparatus driven by a computer-controlled stepping motor (ST-140; Strex) in an atmosphere of 5% CO_2 and 95% air at 37^{o}C as described previously. Briefly, one end of the PDMS pattern was attached to a fixed frame, while the other end was attached to a movable frame. Other two sides were free to move. The movable frame was connected to a motor driven shaft whose amplitude and frequency of stretch was controlled by a programmable microcomputer. Twelve hours prior to stretching, cells were brought to a quiescent state by incubation in Dulbecco's modified Eagle's medium (DMEM)/F-12 culture medium (Invitrogen, Carlsbad, CA, USA) with 0.03% FBS. The relative elongation of the PDMS pattern was uniform across the whole membrane area, and lateral contraction did not exceed 3% at 20% stretch. The cells incubated under a static condition on the PDMS surface were used as a time-matched control. The effect of cyclic uniaxial stretch (0-2h) on the orientation of human airway smooth muscle (HASM) cells has been examined.

The following modeling plans were provided by Jia Hu, a graduate student whom I work with in the lab:

Plan

Modeling cell seeding process

The cell-surface interaction under shear flow will be studied through computational modeling. The IFEM will be combined with adhesion kinetics to study the attachment and detachment process of endothelial cells on PDMS surfaces.

The ligand-receptor binding kinetics will be coupled with FEM to study the cell attachment to PDMS surface under shear flow. In FEM, the fluid dynamics (Navier-Stocks equation) is described by a fixed Eulerian coordinates and particle motion is described in Lagrangian coordinates without the traditional burden of mesh-updating. An Eulerian-Lagrangian mapping is used to exchange information between the two coordinates. When a cell approaches the PDMS surface, ligands on the cell membrane form bonds with receptors on the surface, as demonstrated in Fig. 7. Dembo, et al. proposed an adhesion kinetic equation, where the bond density N_b is calculated as:

$$\frac{\partial N_b}{\partial t} = k_f (N_l - N_b)(N_r - N_b) - k_r N_b , \qquad (1)$$

Where N_l and N_r are the ligand and receptor densities; k_r and k_f are the reverse and forward reaction rates, respectively, and are functions of bond lengths:

$$k_r = k_r^0 \exp\left(-(k_s - k_{ts})L^2 / 2B_z\right),\ k_f = k_f^0 \exp\left(-k_{ts} L^2 / 2B_z\right).$$

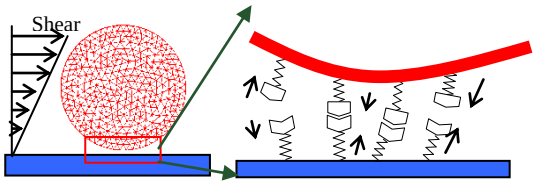

Fig. 7. Ligand-receptor binding dynamics

This reaction model represents a conservation equation of the different species (ligands, receptors, and bonds). The receptor-ligand bonds are modeled as springs with spring constant σ and equilibrium length λ, thus the bond forces are described as a function of bond length L as:

$$f_L = \sigma(L - \lambda) , \qquad (2)$$

The ligand-receptor bond forces can be accumulated on FEM element surface through an integration over the cell surface: $\boldsymbol{\sigma}^s \cdot \mathbf{n} = \int f_L(X^c) d\Gamma$. Such an adhesion force is coupled with the fluid-structure interaction force in the IFEM formulation. A similar adhesion model has been used by Chang et al. and Dong et al. in the study of white blood cell rolling.

Fig. 8 shows a simulation of the attachment of three cells. Cells transported in a flow stream diffuse toward the wall, and finally contact and adhere to the wall due to the adhesive bonds formed between integrins on cell surface and RGDs on coated surface.

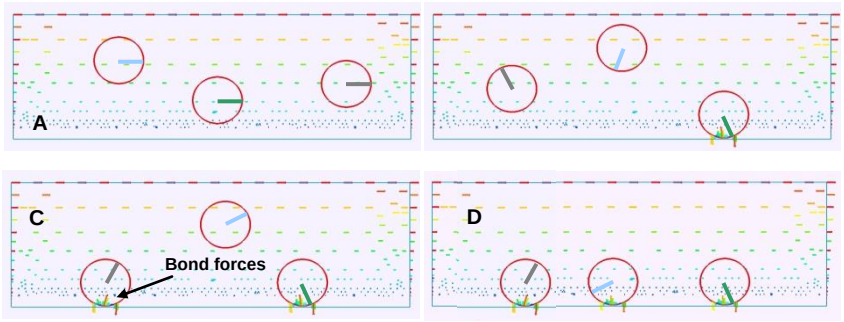

Fig.8. Attachment of three cells under shear flow

Modeling cell spreading and orientation process

Eq. 1 only describes the passive formation/breakage of adhesive bonds. Thus it is only applicable to the cell attachment process, but not spreading and detachment. Active adhesion

and focal adhesion remodeling are more important for cell spreading on the ECM, and response to external mechanical stimuli. In models available in literature, the adhesion remodeling is not associated with external stimulating force such as shear flow. A model that includes focal adhesion remodeling, active and passive forces are required to predict the cell shape change during detachment and under shear flow. As described earlier, a molecular level description of focal adhesion signaling is not possible with available information from molecular biology. Thus, we propose to add signaling in the form of empirical kinetic rate laws that govern the active forces in continuum mechanical description of the cell motion. We will extend Novak et al.'s work to model focal adhesions as clusters of transmembrane proteins tightly connected to the cytoskeleton, but still capable of motion. A simple model is used here to describe the adhesion activation and remodeling process. In this model, the formation of the initial focal adhesion is described as a random process with a rate in proportional to local integrin density. The growth of the focal adhesion is described as an integrin assembly process depending on local stress and other factors, accompanying with stress fiber nucleation. The disassembly of focal adhesion is described by two ways: a passive way of bond breaking if the force exceeds a certain threshold; and active disassembly at certain rate controlled by cell signals. In Fig. 9, the momentum equation for the effective behavior of the cell material is:

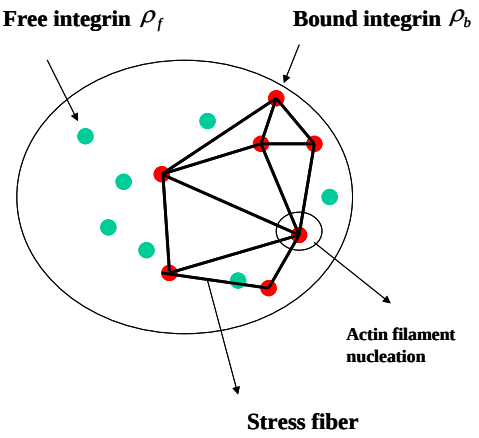

Fig. 9. Model for focal adhesion dynamics of an endothelial cell

$$\rho \frac{D\mathbf{u}}{Dt} = \nabla \cdot \boldsymbol{\sigma} = \nabla \cdot \boldsymbol{\sigma}_{pass} + \nabla \cdot \boldsymbol{\sigma}_{act} \quad (3)$$

where ρ is the material density, $\mathbf{u}$ the velocity field, $\boldsymbol{\sigma}_{pass}$ the passive stress in the material, $\boldsymbol{\sigma}_{act}$ the active stress and $\boldsymbol{\sigma}$ the total stress. The passive stress is the response of the material to the imposed flow e.g. shearing, which depends on the viscoelastic material properties of the fluid and the cell. The active stress directly depends on the active processes, e.g., the stress generated by the stress fibers. For simplicity, we describe stress fibers and integrins in terms of their densities and concentrations. Adhesions will be expressed as the local density of the integrins bound to RGDs, ρ_f. According to experiments, this density increases in proportion to the magnitude of the local force per unit area generated at the adhesion sites by stress fibers, and the local concentration of unbound integrins, ρ_b. Thus, adhesions are assumed to disassemble with a constant rate k_{off_a} and grows at a constant rate k_{on_a}, and is proportional to the force applied on it. Unbound integrins are free to diffuse in cell membrane with a diffusion coefficient D. The corresponding governing equation is:

$$\frac{\partial \rho_b}{\partial t} = (k_0 + k_{on\_a} |\mathbf{F}|)\rho_f - k_{off\_a}\rho_b \quad (4)$$

$$\frac{\partial \rho_f}{\partial t} = -(k_0 + k_{on\_a} |\mathbf{F}|)\rho_f + k_{off\_a}\rho_b + \mathbf{u} \cdot \nabla \rho_f + D\nabla^2 \rho_f \quad (5)$$

where $|\mathbf{F}|$ is the magnitude of the local force. Eqs. (4) and (5) represent the conservation of bounded and unbounded integrins.

The force generated by a stress fiber growth is proportional to the size of the adhesion area. Assuming that force generated by a single stress fiber is f_0, which grows at rate k_f, the stress

fiber dissembles at rate k_{off_s}, and isotropic nucleation of stress fibers is centered at adhesion sites, we have:

$$\frac{\partial \mathbf{F}}{\partial t} = k_f f_0 \rho_b \int_\Gamma \rho_b(\mathbf{x}) \frac{\mathbf{x}-\mathbf{X}}{|\mathbf{x}-\mathbf{X}|} d\Gamma - k_{off\_s}\mathbf{F} \quad (6)$$

The surface integration $f_0\rho_b \int_\Gamma \rho_b(\mathbf{x}) \frac{\mathbf{x}-\mathbf{X}}{|\mathbf{x}-\mathbf{X}|} d\Gamma$ represents the force induced by the stress fibers initiating from X and linking to other adhesion sites. This integration is small at the center of the cell (balanced by the isotropic distribution of focal adhesion sites) and is larger at the edge. This indicates that the adhesion and stress are concentrated at edge.

The governing equations described above are combined with the boundary conditions:

$$\boldsymbol{\sigma}\cdot\mathbf{n} = \mathbf{f}_{ext} \;\&\; \boldsymbol{\sigma}\cdot\mathbf{n} = \rho_b \mathbf{f}_{b0} \quad (7)$$

where f_{b0} is the force generated by a "unit" integrin. The boundary conditions include the traction boundary induced by the external force $\mathbf{f}_{ext}$ (such as the shear force generated by shear flow), and the adhesion force $\rho_b \mathbf{f}_{b0}$ generated at the cell-substrate interface.

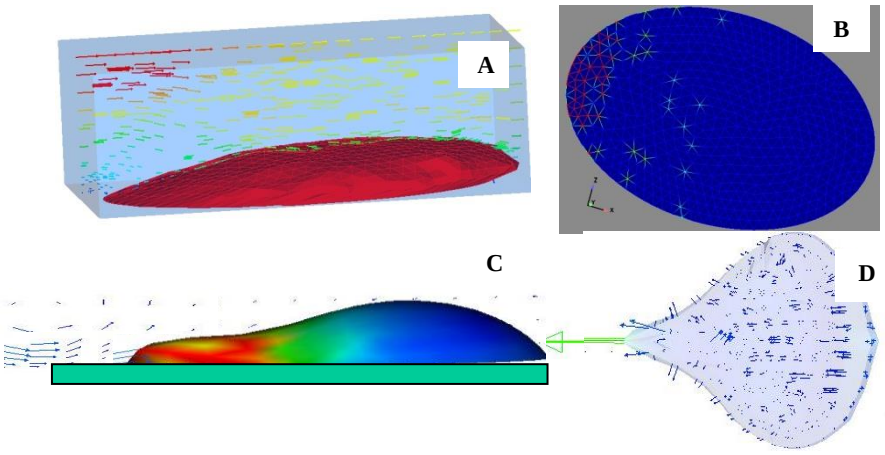

Fig.10. Modeling endothelial cell detachment under shear flow. (A) 3D view of an endothelial cell; (B) Adhesion sites distribution, the color indicates adhesion strength; (C) Side view of cell deformation and flow field; (D) Top view of deformed cell before detachment

Preliminary results of the detachment process for an endothelial cell under shear flow are shown in Fig. 11. Fig. 10A and 10B are the initial cell shape and focal adhesion distribution under a shear flow of 10 Pa. The focal adhesion sites are initiated at the edge of the cell facing incoming flow where forces develop. Fig. 10C and 10 D are deformed cell shapes in side view and top view during detachment. In summary, we will develop a model that includes the active remodeling of focal adhesions, generation of active force, and response to external force. This model will used to model the detachment of endothelial cell under shear from 1 Pa to 10 Pa.

Adhesion probability and distribution

The prediction of the distribution of adhered cells under shear flow *in vitro or in vivo* is important for evaluation of seeding quality. To get a fast evaluation of the attachment and detachment of a large number of cells, it is necessary to get the adhesion probability of an endothelial cell under shear flow. For a simple particles attached to a substrate through ligand-receptor binding, the steady state probability of adhesion P_a is can be characterized by probabilistic kinetic formulation of McQuarrie:

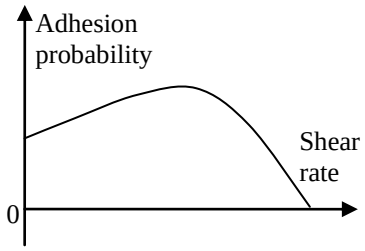

Fig.11 Adhesion probability as a function of shear rates.

$$P_a = m_r m_l K_a^o A_c \exp\left[-\frac{\lambda F_{dis}}{k_B T m_r A_c}\right] \quad (8)$$

Where m_r is the surface density of receptors, m_l the ligand density on particle surface, A_c the contact area of particle, k_BT the thermal energy of system, λ the characteristic length of ligand-receptor bond, and K_a^o the affinity constant of ligand-receptor pair at zero load. F_{dis} is the dislodging force due to hydrodynamic forces, which is comprised of drag force along the flow direction F and torque T.

The adhesion probability of an endothelial cell under different shear rates will be determined by calculating the drag and torque on the deformed cell from the immersed finite element model. Fig. 11 illustrates a rough adhesion model prediction, which shows that the adhesion probability increases first and then decreases with respect to the shear rate increase. The increased adhesion probability is due to the enhanced focal adhesion under slight shear, while adhesion sites are broken under acute shear.

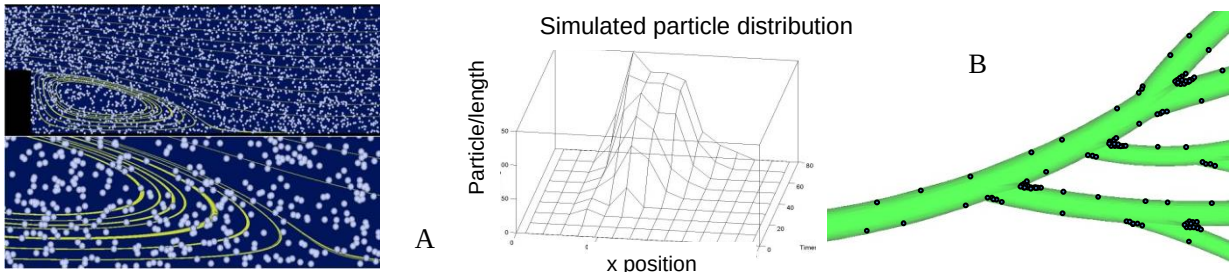

Fig.12. Multi-cell deposition and spatial distribution simulation (A) Cell deposition and distribution plot near the expansion of an artery; (B) Cell deposition in a

The developed adhesion model will be running under parallel clusters to simulate the adhesion and detachment dynamics of thousands of cells, under vessels of various size and flow rates. Fig. 12A illustrates some preliminary results of cell adhesion near a vessel expansion and in branched vessels. To allow large scale simulation, the cell-wall interaction is coarse-grained into a shear rate dependent probability described in Eq. 6. The similar coarse scale models have been applied by the PI to study the aggregation of red blood cells, the deposition of platelets on injured vessels, and the DNA-nanopore interaction. The simulated cell adhesion distribution can be quantitively compared with experimental measurements. We will apply the developed tool to model the adhesion and detachment distribution of endothelial cells under different flow rates.

The following goals will be achieved in this section: (1) shear rate dependent cell adhesion probability and distribution will the modeled and compared with experiments; (2) under the same shear rate, the fraction of cells adhered on the coated wall surface versus that adhered on non-coated control surface and the cells left in flow stream will be determined. This goal is achieved by selectively patterning a certain region of the flow channel with a RGD coating. From Eq. (8), the receptor coating density will largely influences the adhesion probability, and such effect will be verified by using RGD coating of different densities. The number of detached cells will be obtained by counting the number of cells left in the flow stream after several circulations. Periodic boundary condition will be used in the simulation.